Supporting Information

Identifying efficient dynamic tuberculosis case-finding policies for HIV/TB co-epidemics

Reza Yaesoubi[1,2,3] and Ted Cohen[1,2,3]

[1] Department of Epidemiology and the Center for Communicable Disease Dynamics, Harvard School of Public Health, Boston, MA

[2] Division of Global Health Equity, Brigham and Women's Hospital, Boston, MA

[3] Harvard Medical School, Boston, MA

S1 Additional model details

In our model, a person who presents with TB symptoms is tested upon arrival to a health center; if the diagnostic test confirms TB, the patient is referred for TB treatment. Patients who adhere with the referral receive treatment immediately. Non-adherent patients (i.e. initial treatment defaulters) return to infectious states, from which they may visit the health provider again. If the diagnostic test result is (falsely) negative, the individual moves to a non-referring infectious state. If the test result is falsely positive, the individual who adheres with the referral receives treatment, incurs costs but experiences no positive or negative health effects. Successfully treated cases are non-infectious once they begin treatment. Individuals in infectious states may also exit these states by tuberculosis-related death or self-recovery (i.e. recovery without treatment) and transition to the compartment of slow latent progression. Births occur at a rate proportional to the population size and all newborns enter into the susceptible compartment.

HIV co-infection alters the natural history of TB in several ways. HIV−infected individuals have a higher probability of progressive TB upon initial infection [8, 16], a higher probability of progression from latent infection to active TB [5], a lower probability of smear-positivity given active disease [7, 9, 11], and higher mortality rates [7, 13, 19]. To capture the impact of HIV infection, each compartment in Fig. 1 (in the main text) represents two sub-compartments: one for HIV seronegative individuals and one for HIV seropositive individuals [14].

In most regions with high TB prevalence, TB diagnosis relies primarily on sputum smear microscopy which has limited sensitivity, especially among HIV−infected patients [7, 9, 11]. Recently, the Xpert MTB/RIF automated DNA test has been introduced which provides rapid and sensitive detection of TB. A single Xpert MTB/RIF test has been shown to identify $> 98\%$ of patients with smear-positive and TB and $> 70\%$ of patients with smear-negative TB [2, 3, 17]. In our model, we do not consider traditional culture-based diagnosis since it is relatively costly and many resource-limited regions lack the laboratory capacity to perform culture testing at high volume.

In this model, ICF acts to detect, diagnose, and treat symptomatic infectious individuals at a higher rate than under PCF. We assume that when PCF is employed, non-referring infectious individuals do not seek care voluntary, whereas when ICF is in effect, individuals in these states may be diagnosed and treated.

To determine the projected impact of ICF on the TB epidemic, we assume that on average 15% of the population will have access to diagnosis through ICF in any given month that the ICF intervention is employed. This implies that each population member may be exposed to the ICF intervention (e.g., the mobile vans circulating in community) by the end of the ICF period with probability 0.15. At this coverage level, the annual rate of departure from the symptomatic infectious compartments increases by approximately $12 \times 0.1625 = 1.9502$ per year (since $1 - e^{-0.1625} \simeq 0.15$).

A previous study of ICF on TB in Harare, Zimbabwe [6] found that one course of ICF to screen 55,741 individuals was completed in 24 weeks using one mobile van. We estimate that approximately 210 mobile vans would be necessary to achieve 15% coverage level in providing access to diagnosis through ICF in Zimbabwe with population of 13 million individuals ($13,000,000 \times 0.15 \times \frac{24}{55,741 \times 4} \approx 210$, assuming 4 weeks in each month). Assuming that the cost of renting one mobile van and hiring two public health workers to perform screening is \$150 per day, one course of ICF would cost \$31,500 per day in order to be completed by one month at 15% coverage level. Similarly, we estimate one course of ICF at the service level 15% would cost \$9,600 per day in Central African Republic. We note that these resource needs and costs are crude and made simply to illustrate the use of this model framework.

Table S1. Model Calibration

	Zimbabwe			Central African Republic		
Measure	**Model Result**	**Target Estimate**	**Source**	**Model Result**	**Target Estimate**	**Source Source**
TB Prevalence	0.42%	0.39%	[21]	0.43%	0.43%	[21]
HIV Prevalence	14.60%	14.30%	[18]	4.80%	4.70%	[18]
TB Incidence (per 100,000 population)	597	633	[21]	319	327	[21]
Proportion of TB patients with HIV+	0.643	0.75	[21]	0.293	0.33	[21]
Pr{smear+ | HIV+}	0.488	0.48	[10]	0.496	0.48	[10]
Pr{smear+ | HIV−}	0.623	0.65	[20]	0.637	0.65	[20]

S2 Model calibration

To model TB/HIV epidemics, we use the modeling framework proposed in [23] to find the probability distribution of events that may occur (e.g. birth, transmission of infection, or recovery) and then use Monte Carlo simulation to generate epidemic trajectories. We calibrated the model to TB/HIV epidemics in Zimbabwe and Central African Republic. Table 1 compares the results provided by the epidemic models developed here with several target estimates.

S3 Decision model

Let $a_t \in \mathcal{A}$ denote the intervention in effect during the decision period $[t, t+1], t \in \{1, 2, 3, \ldots\}$, where $\mathcal{A}$ is the set of available interventions. In the TB/HIV models considered here, $\mathcal{A} = \{\text{PCF}, \text{ICF}\}$. Let the random variable ξ_t denote the set of events during the decision period $[t, t+1]$ that may trigger an observation, incur costs or lead to change in the population health status or resource availability. Examples of such events include a new infection, hospitalization or death of an infective. Clearly, the decisions in effect during period $[t, t+1]$ will influence the set of events that may occur over this period. For example, in our TB models, ξ_t is a five dimensional vector representing the number of visits to the health care system (incurring diagnosis costs and triggering observations), the number of newly diagnosed TB cases (triggering observations), the number of TB patients starting treatment (incurring treatment costs and change in health status), the number of TB patients recovered from infection (change in health status) and the number of TB deaths (change in health status). While the evolution of the random variable ξ_t over time is not fully observable by the decision maker, we can use mathematical or simulation models to sample from

the stochastic process $X = \{\xi_t, t \geqslant 1\}$.

The policy maker incurs a cost $r(a_t, \xi_t)$ for the decision period $[t, t+1]$ if action $a_t \in \mathcal{A}$ is in effect and the events $\xi_t \in \Xi$ occur during the period $[t, t+1]$. The cost function $r(a_t, \xi_t)$ can be characterized in a variety of ways depending on the policy maker's priorities. For example, if the policy maker wants to minimize the total number of TB cases over the course of epidemic, then cost function $r(a_t, \xi_t)$ can be simply defined as the number of new TB cases during the period $[t, t+1]$. However, efforts to control epidemics may be bounded by the availability of resources, such as antibiotics and budget. In these situations, where both health-related outcomes and the resource consumption level are essential for determining the optimality of a health policy, a more comprehensive cost function is needed. A common approach for defining optimality in these situations is to assume that the policy maker's objective is to maximize the population's net monetary benefit (NMB) [4]. To characterize the cost $r(a_t, \xi_t)$ accordingly, we define the following notation:

- λ: policy maker's willingness-to-pay (WTP) for one unit of health.
- $c(a_t)$: direct cost of implementing the intervention $a_t \in \mathcal{A}$ during the period $[t, t+1]$.
- $q(\xi_t)$: loss in health during period $[t, t+1]$ if random events ξ_t occur.
- $v(\xi_t)$: cost incurred during period $[t, t+1]$ if random events ξ_t occur.

Now, the cost $r(a_t, \xi_t)$, defined as the loss in the population's NMB if action $a_t \in \mathcal{A}$ is in effect and the random events ξ_t occur during the decision period $[t, t+1]$, is calculated by $r(a_t, \xi_t) = \lambda q(\xi_t) + v(\xi_t) + c(a_t)$. We note that the cost function $r(\cdot)$ may also be a function of unobservable events. For example, infectious individuals who are not diagnosed will experience a range of health losses.

During a decision period, the policy maker may obtain observations on different measures. Let $m_t \in \mathcal{M}$ be the observations made during the period $[t, t+1]$ where $\mathcal{M}$ denotes the set of all possible observations during decision periods. For example, in this paper, we assumed that observations can be made on the number of TB cases reported during each decision period and hence $\mathcal{M} = \{0, 1, 2, \ldots\}$. Let h_t denote the history of the epidemic at time index t defined as the sequence of past actions and observations up to the time index t. The history h_t is updated

recursively according to $h_t = \{h_{t-1}, a_{t-1}, m_{t-1}\}$, where h_1 describes the epidemic history prior the time index $t = 1$. Let $\mathcal{H}$ denote the set of all possible values that the history h_t can take. Our objective is to find a policy $\pi : \mathcal{H} \to \mathcal{A}$ that specifies which action to take based on the epidemic history up to a time point $t \in \{1, 2, 3, \ldots\}$ to minimize the expected total discounted loss in net monitory benefit:

$$\mathrm{E}_X[\sum_{t=1}^{T} \gamma^t r(\pi(h_t), \xi_t) | h_1 = \hat{h}_1], \tag{S1}$$

where $\gamma \in (0, 1]$ is the discount rate and $\hat{h}_1$ is the observed history at time index $t = 1$. The expectation in Eq. (S1) is with respect to the stochastic process $X = \{\xi_t, t \geqslant 1\}$ which represents the events occurring over the evolution of the epidemic given the actions $a_t = \pi(h_t), t \in \{0, 1, 2, \ldots\}$. The decision horizon T can be a constant predetermined by the decision maker (e.g., 10 years) or can be a random variable governed by the stochastic process $X = \{\xi_t, t \geqslant 1\}$ (e.g., time when the disease is eradicated).

To find a policy π that minimizes the objective function (S1), we proposed a method using approximate dynamic programming techniques [1, 15]. Readers with limited familiarity with the application of dynamic programming in optimal control of epidemics are referred to [22] for a simple illustrative example.

The proposed method works as follows. For a pair (h_t, a), the Q-value $Q^*(h_t, a)$ is defined as the *optimal* expected total discounted loss in NMB if having observed the epidemic history h_t, the policy maker chooses the action a at time index t. Now, if Q-values $Q^*(\cdot)$ are available, the optimal decision when the history h_t is observed can be found by:

$$a_t^* = \arg\min_{a \in \mathcal{A}} Q^*(h_t, a). \tag{S2}$$

Using Eq. (S2) to make decisions poses two main difficulties. First, finding the optimal Q-values for each history-action pair $(h_t, a) \in \mathcal{H} \times \mathcal{A}$ would be computationally infeasible since the set $\mathcal{H}_t$ can easily be of infinite size. Second, requiring the entire epidemic history to make decision would encumber the successful implementation of the health policies generated by Eq. (S2) in practice.

To overcome these issues, our method uses a *feature-extraction* function $f(\cdot) = (f_1, f_2, \ldots f_K)$ to summarize a given epidemic history h_t into K statistics (or *features*), such as the number of TB

case-notifications or the case finding strategy in effect during the last decision period. The core goal of feature selection is to identify statistics defined within the historical observations of disease spread that can be used to accurately differentiate the current trajectory from the infinite set of possible trajectories. For each action $a \in \mathcal{A}$, the method approximates the Q-values $Q^*(h_t, a)$ with a regression model $\tilde{Q}(f(h_t), a; \theta_a)$, where $f(h_t)$ returns the value of features $(f_1, f_2, \ldots f_K)$ given the history h_t, and θ_a is the vector of regression parameters which should be tuned properly through a training process. For the TB/HIV models considered here, we chose "the case finding intervention in effect during the past decision period" and "TB case notifications during past decision period" as features.

Given approximation functions $\tilde{Q}(\cdot)$ and feature extraction function $f(\cdot)$, the *greedy* policy with respect to the approximation functions $\tilde{Q}(\cdot)$ is then given by:

$$\tilde{\pi}(h) = \arg\min_{a \in \mathcal{A}} \tilde{Q}(f(h), a; \theta_a), \text{ for } h \in \mathcal{H}. \tag{S3}$$

To find the approximation functions $\tilde{Q}(\cdot)$, we propose an *approximate policy iteration* algorithm which is motivated by Lagoudakis and Parr's approach [12] and is modified for systems where states are only partially observable (see Figure 1). The algorithm is an iterative procedure which searches for the optimal policy by generating a sequence of monotonically improving policies. Each iteration of the algorithm consists of two main steps: *policy evaluation* which samples (via simulation) the Q-values and updates (via back-propagation) the approximate Q-functions for the current policy, and *policy improvement* which updates the recommendation for each history $h \in \mathcal{H}$ according to the greedy formula (7) using the new approximate Q-functions.

To explain the steps of the algorithm, let $\tilde{Q}^n(\cdot)$ be the approximate Q-functions at the beginning of iteration $n \geqslant 1$. The *policy improvement* step (see Figure 1) involves characterizing a new policy $\tilde{\pi}^n$ using the greedy formula (S3) with respect to approximate functions $\tilde{Q}^n(\cdot)$. We note that the updated policy $\tilde{\pi}^n$ is not physically stored but it is computed only on demand in policy evaluation step.

In the *policy evaluation* step, we use the epidemic model to obtain a sample on the stochastic process $X = \{\xi_t, t \geqslant 1\}$ and build a sample path which consists of a sequence of history observed at each decision epoch, $\{\hat{h}_1, \hat{h}_2, \hat{h}_3, \ldots, \hat{h}_T\}$, and a sequence of rewards observed during each decision

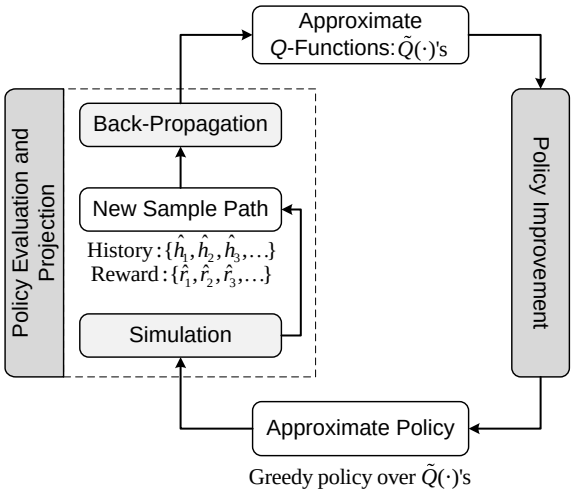

Fig. S1. Approximate Policy Iteration Algorithm

interval, $\{\hat{r}_1, \hat{r}_2, \hat{r}_3, \ldots, \hat{r}_{T-1}\}$. Now, for this sample path, the reward-to-go for the observed history-action pair $(\hat{h}_t, \hat{a}_t)$ is calculated as: $\hat{q}_t = \sum_{\tau=t}^{T-1} \gamma^{\tau-t} \hat{r}_\tau$. In calculating $\hat{q}_t$, we note that if the disease is eradicated at time index T, there is no reward after this time and hence, the sampled reward-to-go at time index T is $\hat{q}_T = 0$. Otherwise, we use $\hat{q}_T = \min_a \tilde{Q}^n(f(\hat{h}_T), a; \tilde{\theta}_a)$ as a sample for reward-to-go at time index $T-1$.

The *policy projection* step in Figure 1 involves a back-propagation algorithm to update the tunable parameters of the approximate Q-functions $\tilde{Q}^n(\cdot)$ using the observed history-action pair $(\hat{h}_t, \hat{a}_t), t \in \{1, 2, 3, \ldots, T\}$ and the corresponding reward-to-go samples $\hat{q}_t, t \in \{1, 2, 3, \ldots, T\}$. For a given decision $a \in \mathcal{A}$, the estimate of the parameter θ_a^n can be updated as:

$$\tilde{\theta}_a^{n+1} \leftarrow \arg\min_\theta \sum_{t=1}^{T} \Big[1_{\{\hat{a}_t = a\}} \big(\hat{q}_t - \tilde{Q}^n(f(\hat{h}_t), a; \theta \big)^2 \Big], \tag{S4}$$

where $1_{\{A\}} = 1$ if A is true and $1_{\{A\}} = 0$, otherwise.

Given the new estimates $\tilde{\theta}_a^{n+1}$, we increment $n \leftarrow n+1$ and repeat the policy improvement step using the updated approximate Q-functions $\tilde{Q}^{n+1}(\cdot)$.

For TB/HIV co-epidemics considered here, we use the modeling framework proposed in [23] to characterize the underlying stochastic process $X = \{\xi_t, t \geqslant 1\}$ which represents events that may occur during an epidemic (e.g. birth, transmission of infections to a susceptible, or recovery). We then use Monte Carlo simulation to sample from the stochastic process X in order to generate

epidemic trajectories. The framework proposed in [23] is a stochastic compartmental model that can be used to represent the within-host natural history of disease, between-host transmission dynamics, and the health care delivery system. As discussed before, other modeling frameworks can also be utilized for this purpose.

For a history-action pair $(h_t, a) \in \mathcal{H} \times \mathcal{A}$, we approximate the Q-value $Q^*(h_t, a)$ with $\tilde{Q}(f(h_t), a; \theta_a)$, where $\tilde{Q}(\cdot; \theta_a)$ is a polynomial function and $f(\cdot)$ is the selected feature-extraction function. We chose a quadratic function to approximate Q-values. Our experiments show that this regression model yield stable and well-behaved policies.

S4 Approximately optimal dynamic case finding policies

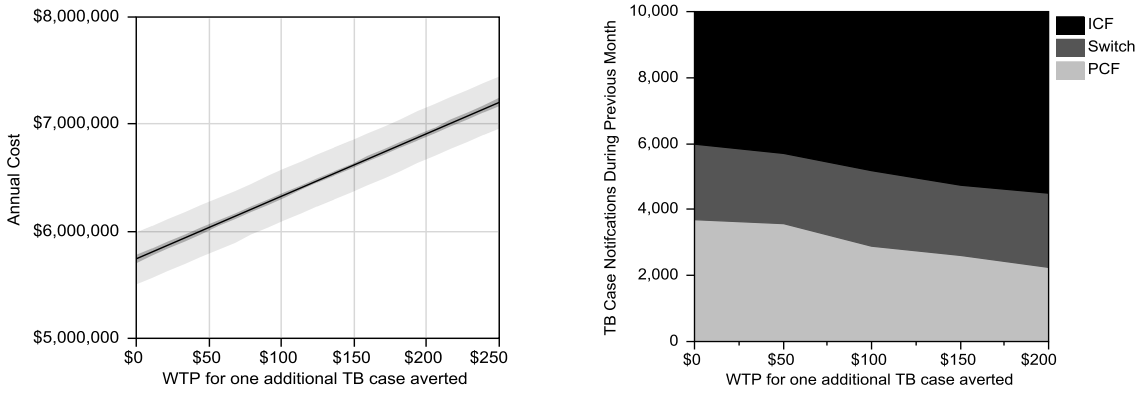

(a) Affordability curve

(b) Decision rule

Fig. S2. Approximately optimal dynamic case finding policies for scenario (1) which resembles the TB/HIV epidemic in Zimbabwe; available TB diagnosis test: sputum microscopy.

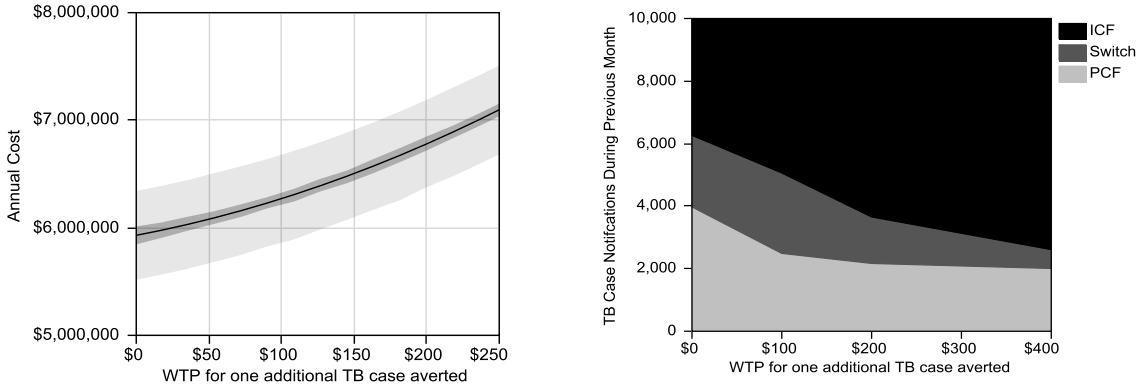

(a) Affordability curve

(b) Decision rule

Fig. S3. Approximately optimal dynamic case finding policies for scenario (2) which resembles the TB/HIV epidemic in Zimbabwe; available TB diagnosis test: sputum microscopy and Xpert MTB/RIF each with 50% coverage.

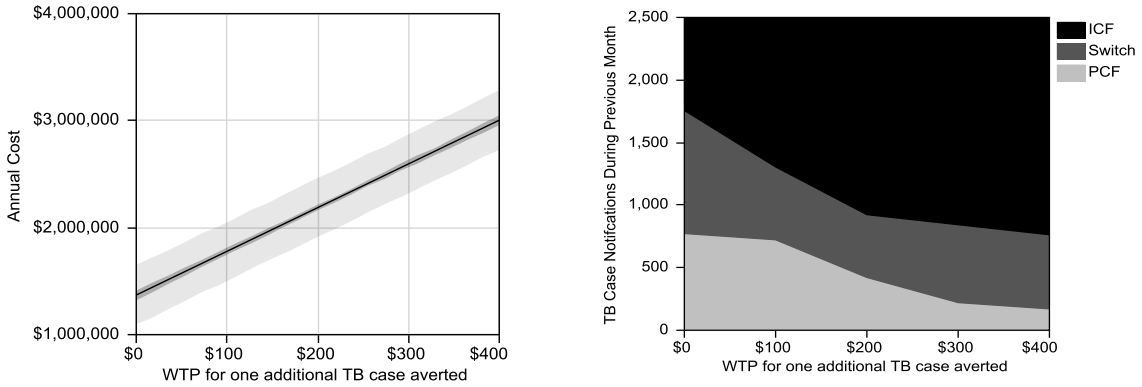

(a) Affordability curve

(b) Decision rule

Fig. S4. Approximately optimal dynamic case finding policies for scenario (3) which resembles the TB/HIV epidemic in Central African Republic; available TB diagnosis test: sputum microscopy.

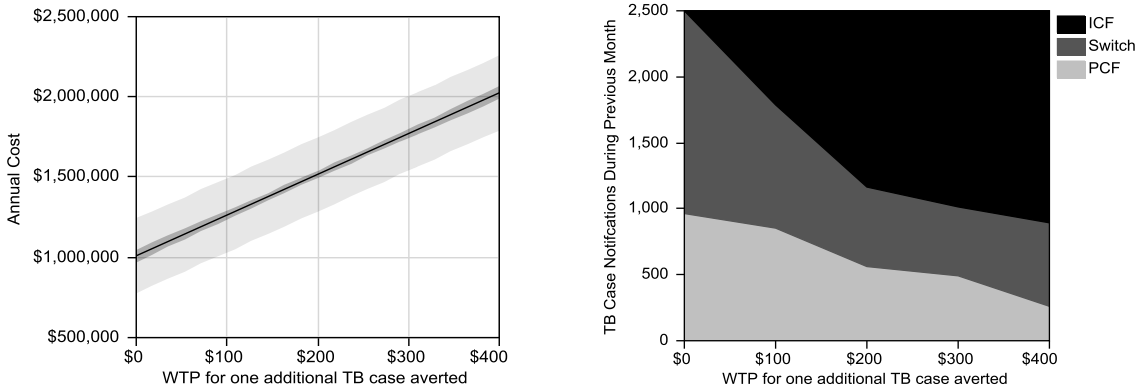

(a) Affordability curve

(b) Decision rule

Fig. S5. Approximately optimal dynamic case finding policies for scenario (4) which resembles the TB/HIV epidemic in Central African Republic; available TB diagnosis test: sputum microscopy and Xpert MTB/RIF each with 50% coverage.

S5 Sensitivity Analysis

This section includes the result of sensitivity analysis on

1. The coverage level (i.e., the average proportion of the population that will have access to diagnosis through ICF in any given month that the ICF intervention is employed) (Figs. S6-S7),

2. The penalty cost (or fixed cost) that may be incurred when we switch from PCF to ICF (Fig. S8), and

3. The delay in reporting of diagnosed TB cases (Figs. S9-S10).

Figs. S6-S7 reveal that comparative benefit of dynamic policies are maintained for different coverage levels of the ICF intervention. Likewise, Fig S8 shows that when switching from PCF to ICF results in a penalty cost, the optimization algorithm generates dynamic policies which outperform static policies that assume the same penalty cost for these switches.

If the number of diagnosed TB cases are reported with a n-month delay, we use the following features to generate dynamic policies: (1) the number of TB case-notifications during the decision period n-months previous and (2) the case finding strategy that was used during this period. Figs. S9-S10 reveal that these delays do not significantly diminish the performance of dynamic case finding policies. The insensitivity of lagged reporting is at least partially attributable to the fact that TB/HIV co-epidemics are relatively stable over this 6-12 month time period. Therefore, the optimization algorithm described above is still able to use these two features to identify dynamic policies which perform reasonably well.

As also described in the main manuscript, the following scenarios were considered.

Scenario (1): resembles the TB/HIV epidemic in Zimbabwe; available TB diagnosis test: sputum microscopy.

Scenario (2): resembles the TB/HIV epidemic in Zimbabwe; available TB diagnosis test: sputum microscopy and Xpert MTB/RIF each with 50% coverage.

Scenario (3): resembles the TB/HIV epidemic in Central African Republic; available TB diagnosis test: sputum microscopy.

Scenario (4): resembles the TB/HIV epidemic in Central African Republic; available TB diagnosis test: sputum microscopy and Xpert MTB/RIF each with 50% coverage.

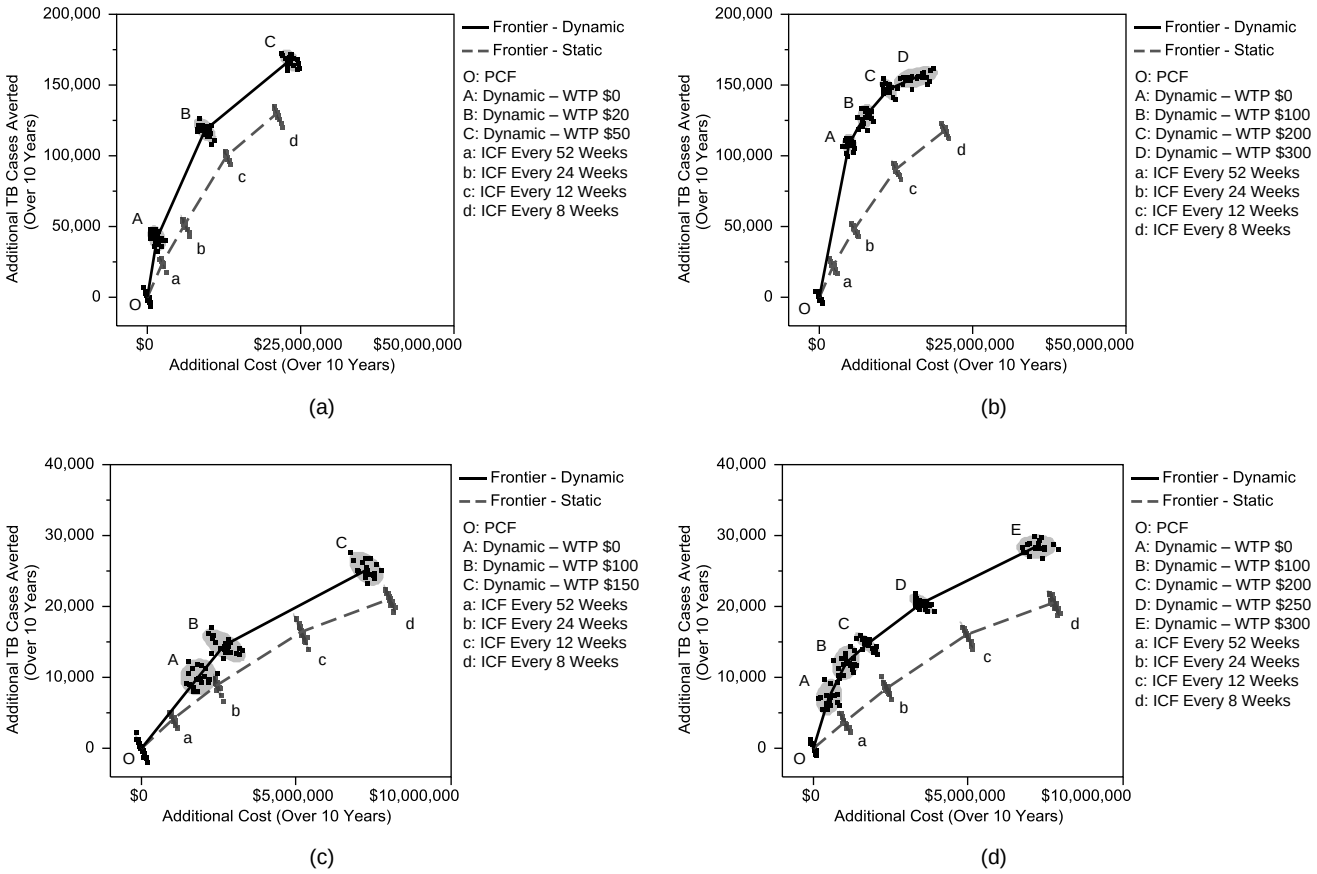

Fig. S6. Cost-effectiveness planes comparing the performance of static versus dynamic ICF policies when on average 10% of the population will have access to diagnosis through ICF in any given month that the ICF intervention is employed. Fig. S6(a)-(d) show the cost-effectiveness planes for scenarios (1)-(4), respectively. The cost-effectiveness frontiers corresponding to dynamic case finding policies strictly dominate the cost-effectiveness frontiers corresponding to static policies for all scenarios.

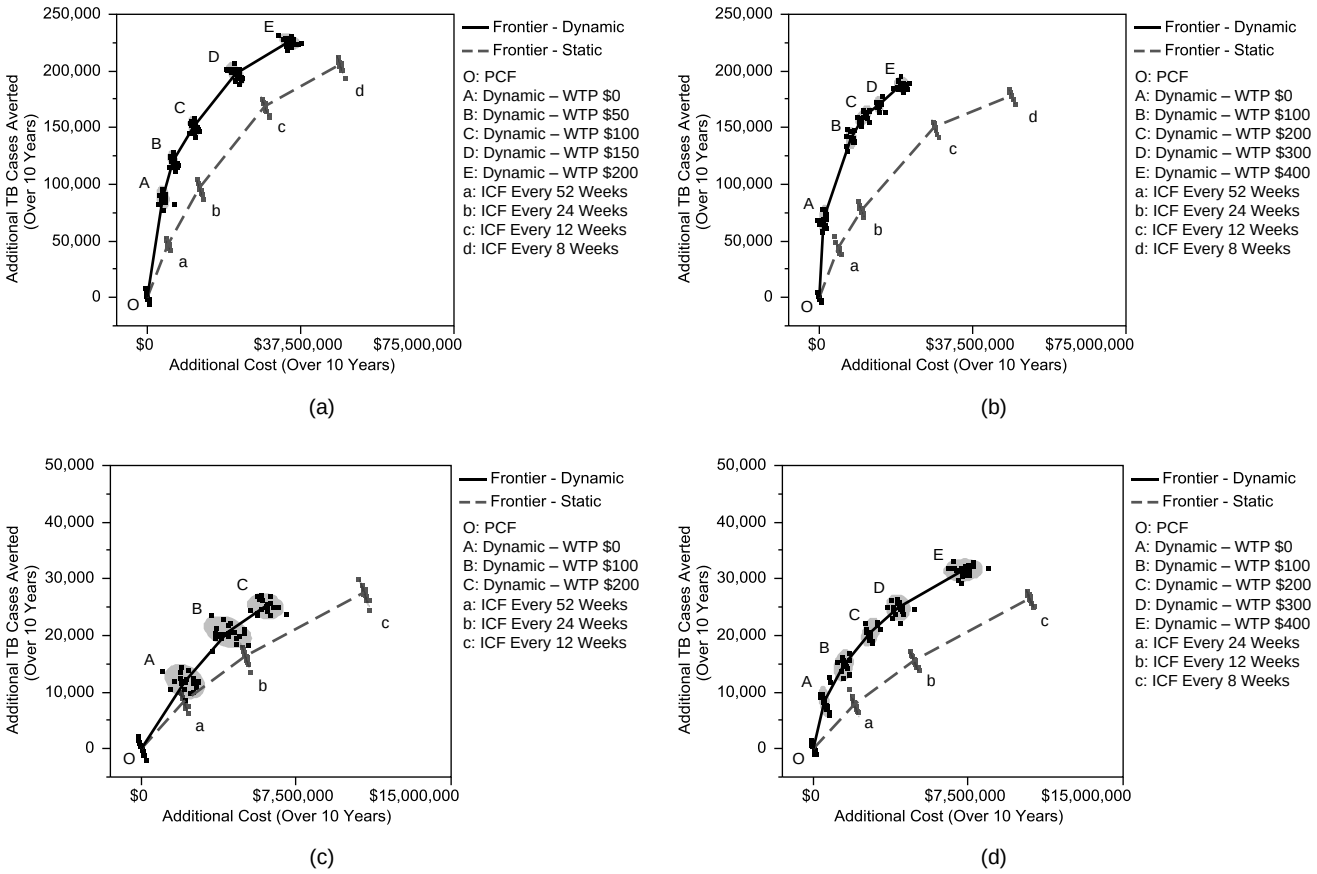

Fig. S7. Cost-effectiveness planes comparing the performance of static versus dynamic ICF policies, when on average 20% of the population will have access to diagnosis through ICF in any given month that the ICF intervention is employed. Fig. S7(a)-(d) show the cost-effectiveness planes for scenarios (1)-(4), respectively. The cost-effectiveness frontiers corresponding to dynamic case finding policies strictly dominate the cost-effectiveness frontiers corresponding to static policies for all scenarios.

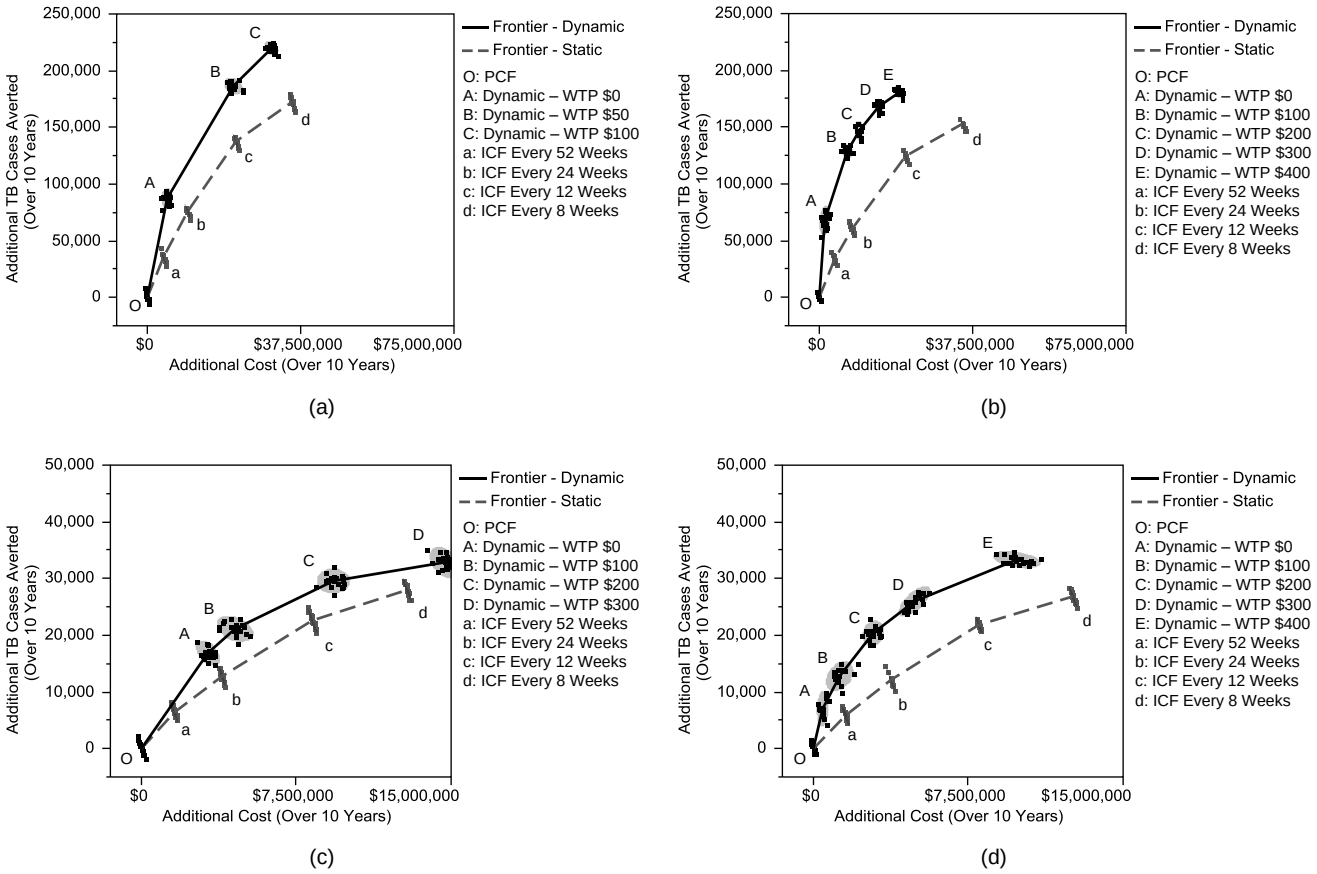

Fig. S8. Cost-effectiveness planes comparing the performance of static versus dynamic ICF policies when on average 15% of the population will have access to diagnosis through ICF in any given month that the ICF intervention is employed and switching from PCF to ICF incurs a penalty cost which is equal to the direct cost of ICF for one month. Fig. S8(a)-(d) show the cost-effectiveness planes for scenarios (1)-(4), respectively. The cost-effectiveness frontiers corresponding to dynamic case finding policies strictly dominate the cost-effectiveness frontiers corresponding to static policies for all scenarios.

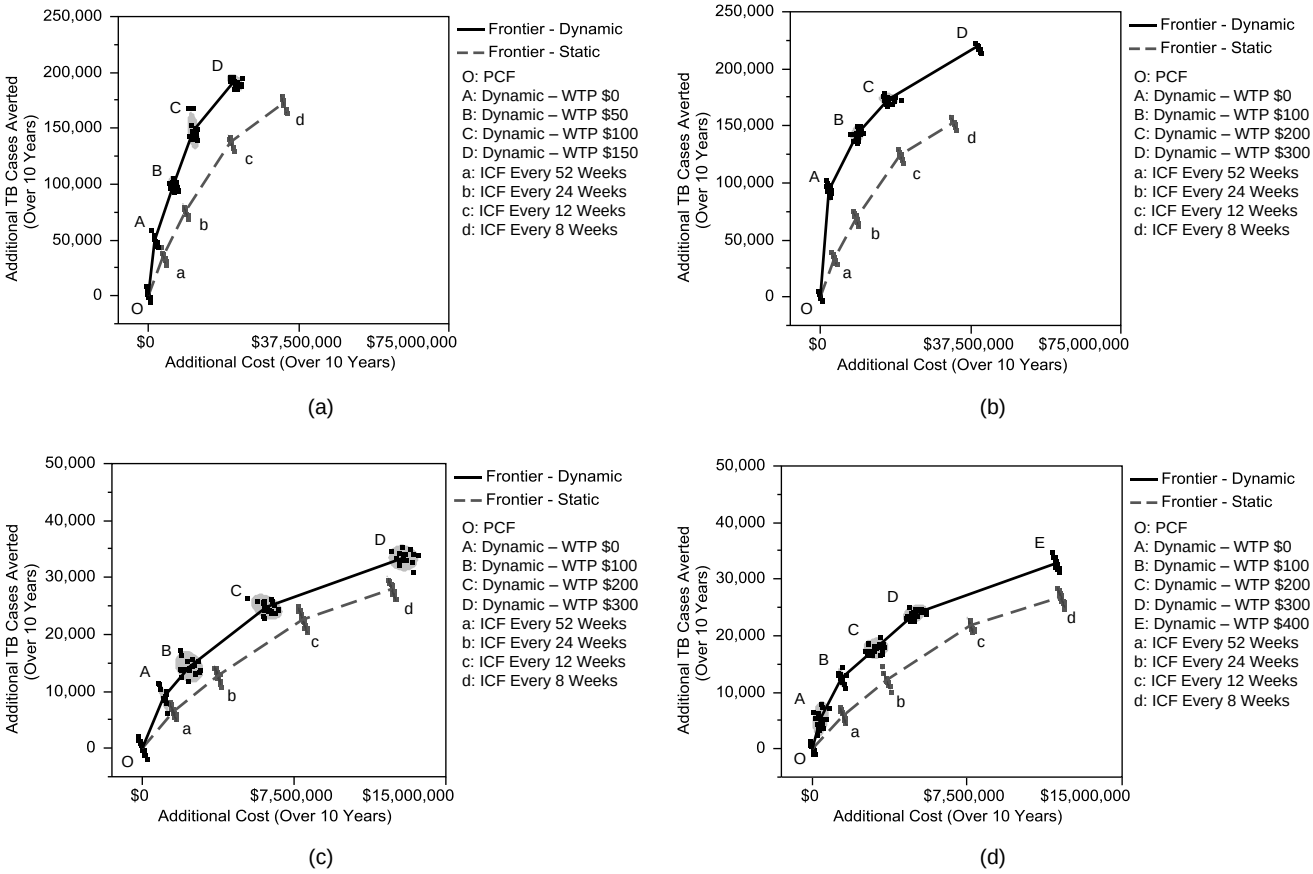

Fig. S 9. Cost-effectiveness planes comparing the performance of static versus dynamic ICF policies when on average 15% of the population will have access to diagnosis through ICF in any given month that the ICF intervention is employed, and the number of TB cases diagnosed during each month become available to the public health decision maker after a 6 month delay. Fig. S9(a)-(d) show the cost-effectiveness planes for scenarios (1)-(4), respectively. The cost-effectiveness frontiers corresponding to dynamic case finding policies strictly dominate the cost-effectiveness frontiers corresponding to static policies for all scenarios.

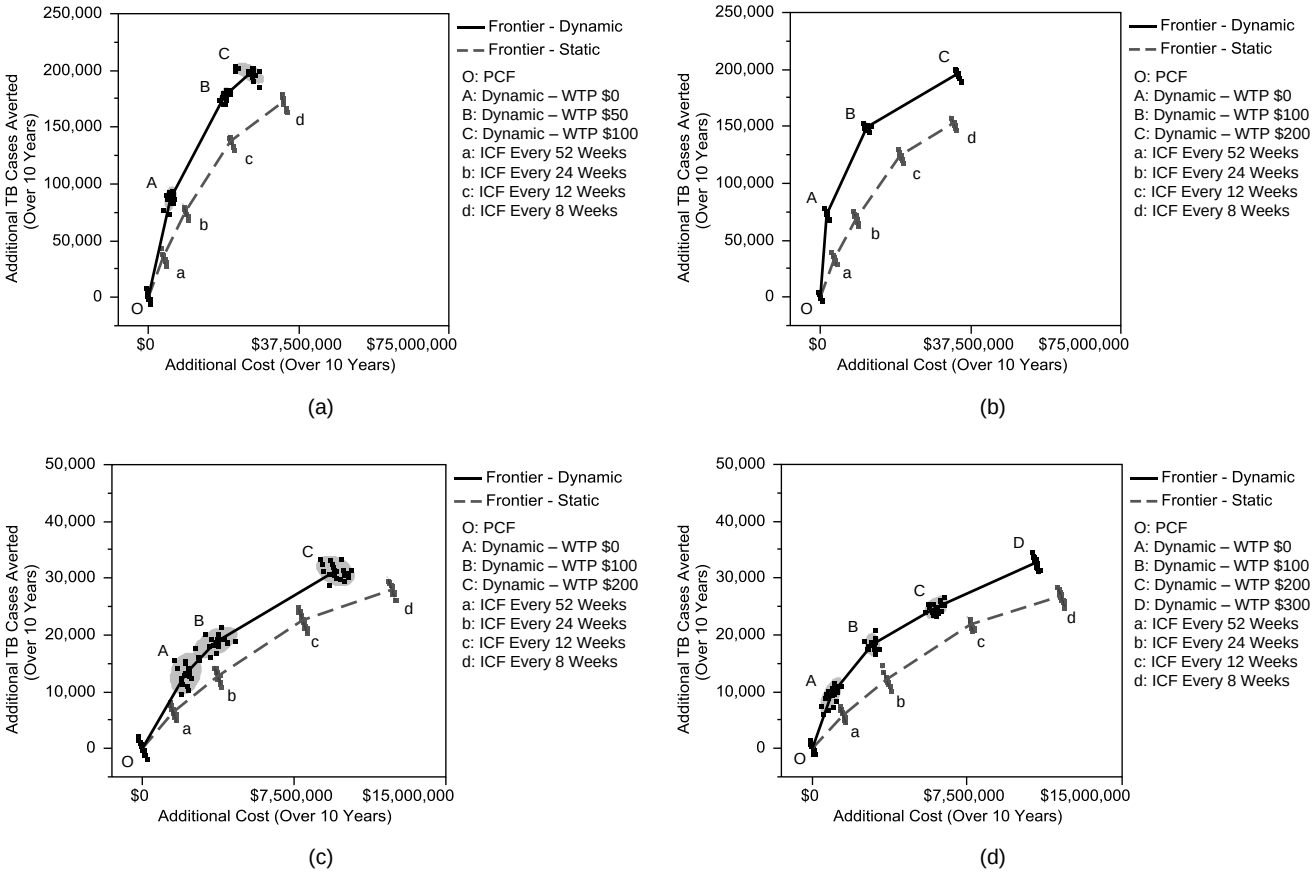

Fig. S10. Cost-effectiveness planes comparing the performance of static versus dynamic ICF policies when on average 15% of the population will have access to diagnosis through ICF in any given month that the ICF intervention is employed, and the number of TB cases diagnosed during each month become available to the public health decision maker after a 12 month delay. Fig. S10(a)-(d) show the cost-effectiveness planes for scenarios (1)-(4), respectively. The cost-effectiveness frontiers corresponding to dynamic case finding policies strictly dominate the cost-effectiveness frontiers corresponding to static policies for all scenarios.

S6 Population's health outcomes for different values of WTP for health

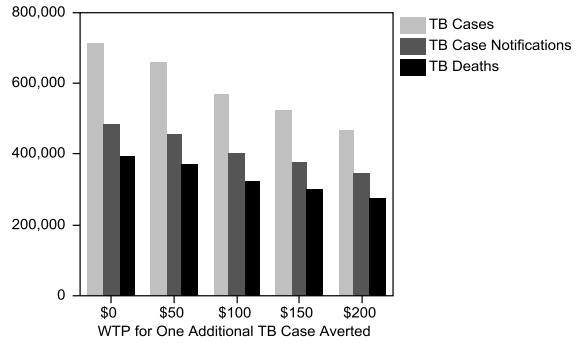

(a) Scenario (1) which resembles the TB/HIV epidemic in Zimbabwe; available TB diagnosis test: sputum microscopy.

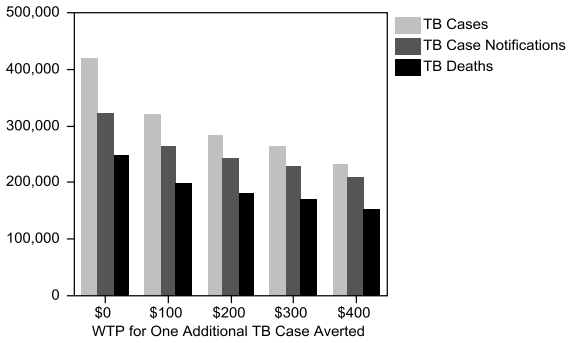

(b) Scenario (2) which resembles the TB/HIV epidemic in Zimbabwe; available TB diagnosis test: sputum microscopy and Xpert MTB/RIF each with 50% coverage.

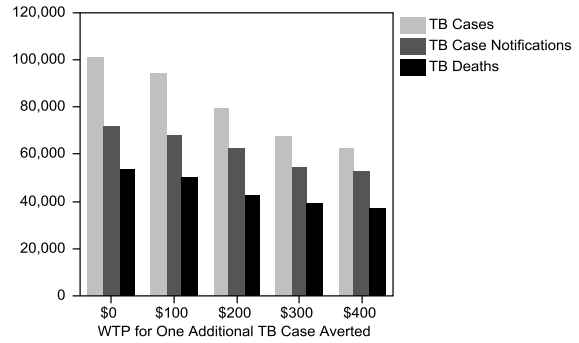

(c) Scenario (3) which resembles the TB/HIV epidemic in Zimbabwe; available TB diagnosis test: sputum microscopy and Xpert MTB/RIF each with 50% coverage.

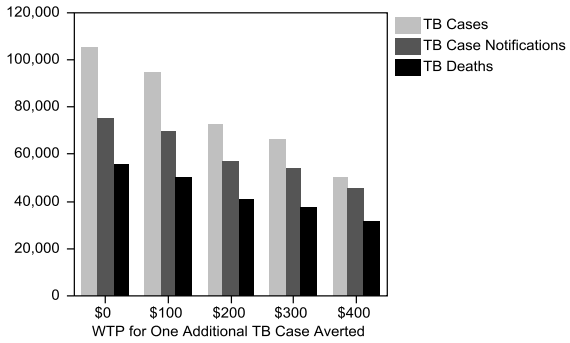

(d) Scenario (4) which resembles the TB/HIV epidemic in Central African Republic; available TB diagnosis test: sputum microscopy and Xpert MTB/RIF each with 50% coverage.

Fig. S 11. Health outcomes for different values of WTP for health over a 10-year horizon. HIV associated TB deaths are counted as TB deaths in these figures.

S7 Switching between PCF and ICF

Fig. S12 compares the number of times that the decision maker should switch between PCF and ICF by following static policies that only specify the frequency of ICF and the dynamic policies shown in §S4. This figure reveals that for the scenarios considered here, for any level of additional health that the decision maker intends to achieve, dynamic policies will require fewer number of switches between PCF and ICF interventions than static policies.

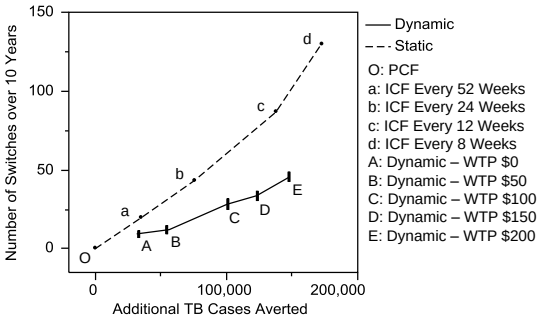

(a) Scenario (1) which resembles the TB/HIV epidemic in Zimbabwe; available TB diagnosis test: sputum microscopy.

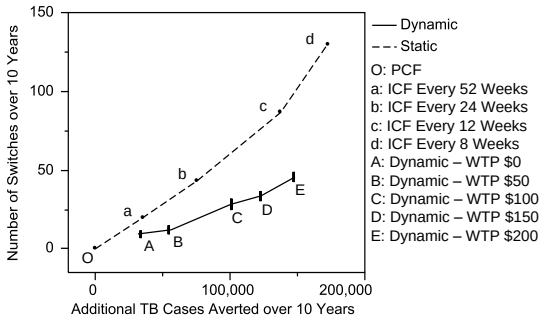

(b) Scenario (2) which resembles the TB/HIV epidemic in Zimbabwe; available TB diagnosis test: sputum microscopy and Xpert MTB/RIF each with 50% coverage.

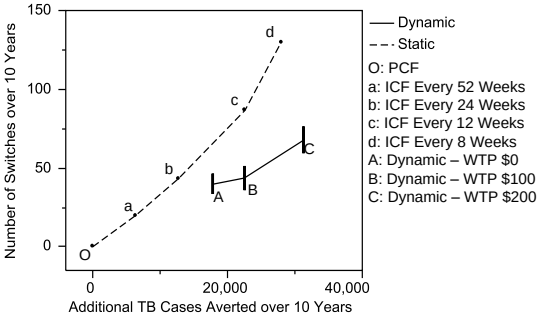

(c) Scenario (3) which resembles the TB/HIV epidemic in Zimbabwe; available TB diagnosis test: sputum microscopy and Xpert MTB/RIF each with 50% coverage.

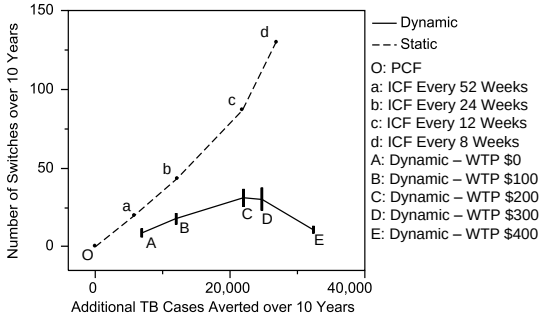

(d) Scenario (4) which resembles the TB/HIV epidemic in Central African Republic; available TB diagnosis test: sputum microscopy and Xpert MTB/RIF each with 50% coverage.

Fig. S12. The number of times that switching between PCF and ICF occurs for static and dynamic policies. Bars around the points corresponding to dynamic policies (denoted with capital letters) represent 95% confidence intervals.

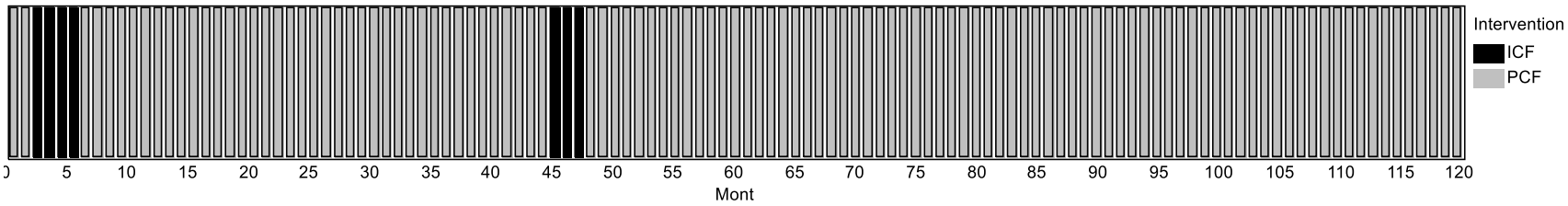

(a) WTP = \$0 per one additional TB cases averted.

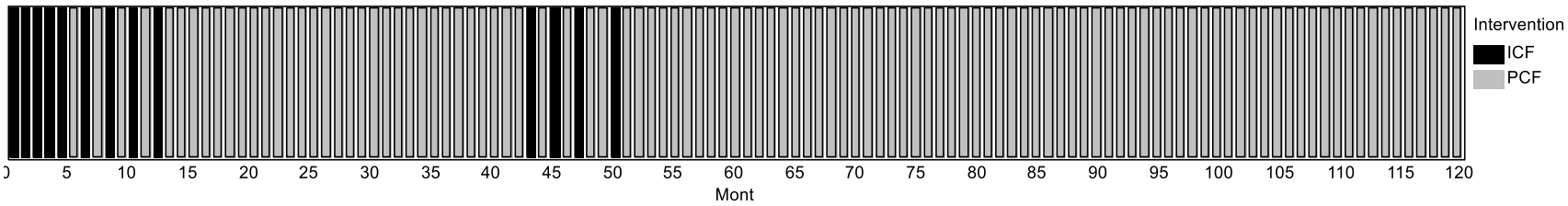

(b) WTP = \$100 per one additional TB cases averted.

Fig. S13. Use of case finding interventions for one trajectory of the TB/HIV epidemic in scenario (1) which resembles the TB/HIV epidemic in Zimbabwe; available TB diagnosis test: sputum microscopy.

S8 Model parameters

Table S2. Parameters of the TB/HIV model - Birth and mortality parameters

Parameters	Zimbabwe	Central African Republic
Annual birth rate	0.033	0.042
Annual natural death rate	0.017	0.0215
Annual death rate for HIV+ individuals	0.024	0.0285
Additional annual mortality rate due to TB in class "Smear-Negative Symptomatic Infectious/Non-Referring" among HIV− individuals	0.317	0.232
Additional annual mortality rate due to TB in class "Smear-Negative Symptomatic Infectious/Non-Referring" among HIV+ individuals	0.517	0.332
Additional annual mortality rate due to TB in class "Smear-Negative Symptomatic Infectious/Self-Referring" among HIV− individuals	0.317	0.232
Additional annual mortality rate due to TB in class "Smear-Negative Symptomatic Infectious/Self-Referring" among HIV+ individuals	0.517	0.332
Additional annual mortality rate due to TB in class "Smear-Positive Symptomatic Infectious/Non-Referring" among HIV− individuals	0.437	0.322
Additional annual mortality rate due to TB in class "Smear-Positive Symptomatic Infectious/Non-Referring" among HIV+ individuals	0.637	0.422
Additional annual mortality rate due to TB in class "Smear-Positive Symptomatic Infectious/Self-Referring" among HIV− individuals	0.437	0.322
Additional annual mortality rate due to TB in class "Smear-Positive Symptomatic Infectious/Self-Referring" among HIV+ individuals	0.637	0.422

Table S3. Parameters of the TB/HIV model - Infectivity parameters

Parameters	Zimbabwe	Central African Republic
Annual HIV infectivity rate[♭]	0.120	0.125
Annual infectivity rate[♭] of class "Asymptomatic Infectious" among HIV− and HIV+	2.063	2.475
Annual infectivity rate[♭] of class "Smear-Negative Symptomatic Infectious/Non-Referring" among HIV− and HIV+	2.75	3.3
Annual infectivity rate[♭] of class "Smear-Negative Symptomatic Infectious/ Self-Referring" among HIV− and HIV+	2.75	3.30
Annual infectivity rate[♭] of class "Smear-Positive Symptomatic Infectious/ Non-Referring" among HIV− and HIV+	12.5	15.0
Annual infectivity rate[♭] of class "Smear-Positive Symptomatic Infectious/Self-Referring" among HIV− and HIV+	12.5	15.0

[♭]Infectivity rate is the expected number of secondary infections per unit of time caused by an infectious individual.

Table S4. Parameters of the TB/HIV model - Latent period parameters

Parameters	Zimbabwe	Central African Republic
Probability of moving to "Fast Latent" class upon infection (HIV−)	0.115	0.115
Probability of moving to "Fast Latent" class upon infection (HIV+)	0.9	0.7
Annual rate of leaving class "Fast Latent" (HIV−)	1.5	1.5
Annual rate of leaving class "Fast Latent" (HIV+)	12.0	12.0

Table S5. Parameters of the TB/HIV model - Infectious classes' parameters

Parameters	Zimbabwe	Central African Republic
Annual rate of leaving class "Asymptomatic Infectious" (HIV−)	2.0	2.0
Annual rate of leaving class "Asymptomatic Infectious" (HIV−)	10.0	10.0
Annual transition rate from "Smear-Negative Symptomatic Infectious/Non-Referring" to "Smear-Negative Symptomatic Infectious/Self-Referring" among HIV− individuals	2.5	2.5
Annual transition rate from "Smear-Negative Symptomatic Infectious/Non-Referring" to "Smear-Negative Symptomatic Infectious/Self-Referring" among HIV+ individuals	4.0	4.0
Annual transition rate from "Smear-Negative Symptomatic Infectious/Non-Referring" to "Smear-Positive Symptomatic Infectious/Non-Referring" among HIV− individuals	3.5	3.5
Annual transition rate from "Smear-Negative Symptomatic Infectious/Non-Referring" to "Smear-Positive Symptomatic Infectious/Non-Referring" among HIV+ individuals	5.0	5.0
Annual transition rate from "Smear-Negative Symptomatic Infectious/Self-Referring" to "Smear-Positive Symptomatic Infectious/Self-Referring" among HIV− individuals	3.5	3.5
Annual transition rate from "Smear-Negative Symptomatic Infectious/Self-Referring" to "Smear-Positive Symptomatic Infectious/Self-Referring" among HIV+ individuals	5.0	5.0
Annual transition rate from "Smear-Positive Symptomatic Infectious/Non-Referring" to "Smear-Positive Symptomatic Infectious/Self-Referring" among HIV− individuals	2.0	2.0
Annual transition rate from "Smear-Positive Symptomatic Infectious/Non-Referring" to "Smear-Positive Symptomatic Infectious/Self-Referring" among HIV+ individuals	7.0	7.0

Table S6. Parameters of the TB/HIV model - Cure parameters

Parameters	Zimbabwe	Central African Republic
Annual natural cure rate in "Smear-Negative Symptomatic Infectious/Non-Referring" among HIV− individuals	0.3	0.3
Annual natural cure rate in "Smear-Negative Symptomatic Infectious/Self-Referring" among HIV+ individuals	0.1	0.1
Annual natural cure rate in "Smear-Negative Symptomatic Infectious/Self-Referring" among HIV− individuals	0.3	0.3
Annual natural cure rate in "Smear-Negative Symptomatic Infectious/Self-Referring" among HIV+ individuals	0.1	0.1
Annual natural cure rate in "Smear-Positive Symptomatic Infectious/Non-Referring" among HIV− individuals	0.19	0.19
Annual natural cure rate in "Smear-Positive Symptomatic Infectious/Non-Referring" among HIV+ individuals	0.0	0.0
Annual natural cure rate in "Smear-Positive Symptomatic Infectious/Self-Referring" among HIV− individuals	0.19	0.19
Annual natural cure rate in "Smear-Positive Symptomatic Infectious/Self-Referring" among HIV+ individuals	0.0	0.0
Annual cure rate in "Treatment" among HIV− patients	2.0	2.0
Annual cure rate in "Treatment" among HIV− patients	2.0	2.0

Table S7. Parameters of the TB/HIV model - Referring to health providers

Parameters	Zimbabwe	Central African Republic
Annual rate of visit to health provider from "Smear-Negative Symptomatic Infectious/Self-Referring among HIV− individuals under PCF	3.0	3.0
Annual rate of visit to health provider from "Smear-Negative Symptomatic Infectious/Self-Referring" among HIV+ individuals under PCF	15.0	15.0
Annual rate of visit to health provider from "Smear-Positive Symptomatic Infectious/Self-Referring" among HIV− individuals under PCF	4.0	4.0
Annual rate of visit to health provider from "Smear-Positive Symptomatic Infectious/Self-Referring" among HIV+ individuals under PCF	12.0	12.0
Annual rate of visit to health provider from "Smear-Negative Symptomatic Infectious/Non-Referring" among HIV− individuals under ICF	3.45	3.45
Annual rate of visit to health provider from "Smear-Negative Symptomatic Infectious/Non-Referring" among HIV+ individuals under ICF	3.45	3.45
Annual rate of visit to health provider from "Smear-Negative Symptomatic Infectious/Self-Referring" among HIV− individuals under ICF	6.45	6.45
Annual rate of visit to health provider from "Smear-Negative Symptomatic Infectious/Self-Referring" among HIV+ individuals under ICF	18.45	18.45
Annual rate of visit to health provider from "Smear-Positive Symptomatic Infectious/Non-Referring" among HIV− individuals under ICF	3.45	3.45
Annual rate of visit to health provider from "Smear-Positive Symptomatic Infectious/Non-Referring" among HIV+ individuals under ICF	3.45	3.45
Annual rate of visit to health provider from "Smear-Positive Symptomatic Infectious/Self-Referring" among HIV− individuals under ICF	7.45	7.45
Annual rate of visit to health provider from "Smear-Positive Symptomatic Infectious/Self-Referring" among HIV+ individuals under ICF	15.45	15.45

Table S8. Parameters of the TB/HIV model - Diagnostic test parameters

Parameters	Zimbabwe	Central African Republic
Sensitivity of Xpert MTB/RIF for smear-negative TB patients with HIV− status	0.725	0.725
Sensitivity of Xpert MTB/RIF for smear-negative TB patients with HIV+ status	0.725	0.725
Sensitivity of Xpert MTB/RIF for smear-positive TB patients with HIV− status	0.982	0.982
Sensitivity of Xpert MTB/RIF for smear-positive TB patients with HIV+ status	0.982	0.982
Sensitivity of smear microscopy for smear-negative TB patients with HIV− status	0.0	0.0
Sensitivity of smear microscopy for smear-negative TB patients with HIV+ status	0.0	0.0
Sensitivity of smear microscopy for smear-positive TB patients with HIV− status	1.0	1.0
Sensitivity of smear microscopy for smear-positive TB patients with HIV+ status	1.0	1.0

Table S9. Parameters of the TB/HIV model - Healthcare system parameters

Parameters	Zimbabwe	Central African Republic
Probability of compliance to receive TB treatment	0.95	0.95
Daily cost of TB treatment	$1.00	$1.00
Monthly cost of active case finding	$31,500	$9,600
Cost of Xpert MTB/RIF test	$30.00	$30.00
Cost of smear microscopy test	$5.00	$5.00

References

[1] D. P. Bertsekas and J. N. Tsitsiklis. *Neuro-Dynamic Programming*. Athena Scientific, 1996.

[2] C. C. Boehme, P. Nabeta, D. Hillemann, M. P. Nicol, S. Shenai, F. Krapp, J. Allen, R. Tahirli, R. Blakemore, R. Rustomjee, et al. Rapid molecular detection of tuberculosis and rifampin resistance. *New England Journal of Medicine*, 363(11):1005–1015, 2010.

[3] C. C. Boehme, M. P. Nicol, P. Nabeta, J. S. Michael, E. Gotuzzo, R. Tahirli, M. T. Gler, R. Blakemore, W. Worodria, C. Gray, et al. Feasibility, diagnostic accuracy, and effectiveness of decentralised use of the Xpert MTB/RIF test for diagnosis of tuberculosis and multidrug resistance: a multicentre implementation study. *The Lancet*, 30:1495–1505, 2011.

[4] Andrew Briggs, Karl Claxton, and Mark Sculpher. *Decision Modelling for Health Economic Evaluation*. Oxford University Press, 2006.

[5] H. C. Bucher, L. E. Griffith, G. H. Guyatt, P. Sudre, M. Naef, P. Sendi, and M. Battegay. Isoniazid prophylaxis for tuberculosis in HIV infection: a meta-analysis of randomized controlled trials. *AIDS*, 13(4):501, 1999.

[6] E. L. Corbett, T. Bandason, T. Duong, E. Dauya, B. Makamure, G. J. Churchyard, B. G. Williams, S. S. Munyati, A. E. Butterworth, P. R. Mason, et al. Comparison of two active case-finding strategies for community-based diagnosis of symptomatic smear-positive tuberculosis and control of infectious tuberculosis in Harare, Zimbabwe (DETECTB): a cluster-randomised trial. *The Lancet*, 376(9748):1244–1253, 2010.

[7] E. L. Corbett, C. J. Watt, N. Walker, D. Maher, B. G. Williams, M. C. Raviglione, and C. Dye. The growing burden of tuberculosis: global trends and interactions with the HIV epidemic. *Archives of Internal Medicine*, 163(9):1009, 2003.

[8] C. L. Daley, P. M. Small, G. F. Schecter, G. K. Schoolnik, R. A. McAdam, W. R. Jacobs Jr, and P. C. Hopewell. An outbreak of tuberculosis with accelerated progression among persons infected with the human immunodeficiency virus. *New England Journal of Medicine*, 326(4):231–235, 1992.

[9] A. M. Elliott, B. Halwiindi, R. J. Hayes, N. Luo, G. Tembo, L. Machiels, C. Bem, G. Steenbergen, J. O. Pobee, and P. P. Nunn. The impact of human immunodeficiency virus on presentation and diagnosis of tuberculosis in a cohort study in Zambia. *Journal of Tropical Medicine and Hygiene*, 96(1):1, 1993.

[10] J. M. FitzGerald, S. Grzybowski, and E. A. Allen. The impact of human immunodeficiency virus infection on tuberculosis and its control. *Chest*, 100(1):191–200, 1991.

[11] H. Getahun, M. Harrington, R. O'Brien, and P. Nunn. Diagnosis of smear-negative pulmonary tuberculosis in people with HIV infection or AIDS in resource-constrained settings: informing urgent policy changes. *The Lancet*, 369(9578):2042–2049, 2007.

[12] M.G. Lagoudakis and R. Parr. Least-squares policy iteration. *The Journal of Machine Learning Research*, 4:1107–1149, 2003.

[13] W. Manosuthi, P. Tantanathip, S. Chimsuntorn, B. Eampokarap, S. Thongyen, S. Nilkamhang, and S. Sungkanuparph. Treatment outcomes of patients co-infected with HIV and tuberculosis who received a nevirapine-based antiretroviral regimen: a four-year prospective study. *International Journal of Infectious Diseases*, 14(11):e1013–e1017, 2010.

[14] C. J. L. Murray and J. A. Salomon. Modeling the impact of global tuberculosis control strategies. *Proceedings of the National Academy of Sciences of the United States of America*, 95(23):13881, 1998.

[15] W. B. Powell. *Approximate Dynamic Programming: Solving the Curses of Dimensionality*. Wiley, 2nd edition, 2011.

[16] R. W. Shafer, S. P. Singh, C. Larkin, and P. M. Small. Exogenous reinfection with multidrug-resistant mycobacterium tuberculosis in an immunocompetent patient. *Tubercle and Lung Disease*, 76(6):575–577, 1995.

[17] G. Theron, J. Peter, R. van Zyl-Smit, H. Mishra, E. Streicher, S. Murray, R. Dawson, A. Whitelaw, M. Hoelscher, S. Sharma, et al. Evaluation of the Xpert MTB/RIF assay for the diagnosis of pulmonary tuberculosis in a high HIV prevalence setting. *American Journal of Respiratory and Critical Care Medicine*, 184(1):132–140, 2011.

[18] UNAIDS. *AIDSInfo*. Available via http://www.unaids.org/en/dataanalysis/datatools/aidsinfo/ [Last accessed Jan 1, 2013].

[19] M. A. B. van der Sande, M. F. Schim van der Loeff, R. C. Bennett, M. Dowling, A. A. Aveika, T. O. Togun, S. Sabally, D. Jeffries, R. A. Adegbola, R. Sarge-Njie, et al. Incidence of tuberculosis and survival after its diagnosis in patients infected with HIV-1 and HIV-2. *AIDS*, 18(14):1933, 2004.

[20] E. Vynnycky and P. E. M. Fine. The natural history of tuberculosis: the implications of age-dependent risks of disease and the role of reinfection. *Epidemiology and Infection*, 119(2):183–201, 1997.

[21] World Health Organization. *Tuberculosis Country Profiles*. Available viat http://www.who.int/tb/country/data/profiles/en/index.html [Last accessed Jan 1, 2013].

[22] R. Yaesoubi and T. Cohen. Dynamic health policies for controlling the spread of emerging infections: Influenza as an example. *PLoS One*, 6(9):e24043, 2011.

[23] R. Yaesoubi and T. Cohen. Generalized Markov models of infectious disease spread: A novel framework for developing dynamic health policies. *European Journal of Operational Research*, 215(3):679–687, 2011.